

Naval Surface Warfare Center

Carderock Division

West Bethesda, MD 20817-5700

NSWCCD-61-TR-2013/18

April 2013

Survivability, Structures, and Materials Department

Technical Report

Localized Mechanical Properties of Friction Stir Processed Sensitized 5456-H116 Al

By

Caroline Scheck, Kim N. Tran, and Jennifer Wolk,
(Naval Surface Warfare Center, Carderock Division)

and

Marc Zupan
(University of Maryland, Baltimore County)



Approved for public release; distribution is unlimited

**Naval Surface Warfare Center
Carderock Division**

West Bethesda, MD 20817-5700

NSWCCD-61-TR-2013/18

April 2013

Survivability, Structures, and Materials Department
Technical Report

**Localized Mechanical Properties of Friction Stir
Processed Sensitized 5456-H116 Al**

By

Caroline Scheck, Kim N. Tran, Jennifer Wolk,
(Naval Surface Warfare Center, Carderock Division)
and
Marc Zupan
(University of Maryland, Baltimore County)



Approved for public release; distribution is unlimited

This page intentionally left blank

| REPORT DOCUMENTATION PAGE | | | | Form Approved OMB No. 0704-0188 | |
|--|-----------------------------|------------------------------|---------------------------------------|--|---|
| Public reporting burden for this collection of information is estimated to average 1 hour per response, including the time for reviewing instructions, searching existing data sources, gathering and maintaining the data needed, and completing and reviewing this collection of information. Send comments regarding this burden estimate or any other aspect of this collection of information, including suggestions for reducing this burden to Department of Defense, Washington Headquarters Services, Directorate for Information Operations and Reports (0704-0188), 1215 Jefferson Davis Highway, Suite 1204, Arlington, VA 22202-4302. Respondents should be aware that notwithstanding any other provision of law, no person shall be subject to any penalty for failing to comply with a collection of information if it does not display a currently valid OMB control number. PLEASE DO NOT RETURN YOUR FORM TO THE ABOVE ADDRESS. | | | | | |
| 1. REPORT DATE (DD-MM-YYYY) 09-April-2013 | | 2. REPORT TYPE Final | | 3. DATES COVERED (From - To) - | |
| 4. TITLE AND SUBTITLE Localized Mechanical Properties of Friction Stir Processed Sensitized 5456-H116 Al | | | | 5a. CONTRACT NUMBER N0001411WX21246 | |
| | | | | 5b. GRANT NUMBER | |
| | | | | 5c. PROGRAM ELEMENT NUMBER | |
| 6. AUTHOR(S) Caroline Scheck, Kim N. Tran, Jennifer Wolk (Naval Surface Warfare Center, Carderock Division) and Marc Zupan (University of Maryland, Baltimore County) | | | | 5d. PROJECT NUMBER | |
| | | | | 5e. TASK NUMBER | |
| | | | | 5f. WORK UNIT NUMBER | |
| 7. PERFORMING ORGANIZATION NAME(S) AND ADDRESS(ES) AND ADDRESS(ES) NAVAL SURFACE WARFARE CENTER CARDEROCK DIVISION (CODE 61) 9500 MACARTHUR BOULEVARD WEST BETHESDA, MD 20817-5700 | | | | 8. PERFORMING ORGANIZATION REPORT NUMBER NSWCCD-61-TR-2013/18 | |
| 9. SPONSORING / MONITORING AGENCY NAME(S) AND ADDRESS(ES) OFFICE OF NAVAL RESEARCH CODE 332 (DR. WILLIAM MULLINS) 875 N. RANDOLPH STREET ARLINGTON, VA 22203 | | | | 10. SPONSOR/MONITOR'S ACRONYM(S) | |
| | | | | 11. SPONSOR/MONITOR'S REPORT NUMBER(S) | |
| 12. DISTRIBUTION / AVAILABILITY STATEMENT Approved for public release; distribution is unlimited. | | | | | |
| 13. SUPPLEMENTARY NOTES | | | | | |
| 14. ABSTRACT The microstructures of Al-Mg alloys with greater than 3wt.% Mg can sensitize leaving the material susceptible to intergranular corrosion (IGC); sensitized microstructures are identified by the amassing of □ phase precipitates at grain boundaries. Friction stir processing (FSP) has previously been shown to increase the corrosion resistance of sensitized Al-Mg alloys through break-up of the continuous network of □ phase particles ^[1] . In this study, multi-pass FSP is applied to a sensitized 5456-H116 aluminum plate and the resulting microstructure is linked to local mechanical properties (0.2% yield strength, ultimate tensile strength, and elongation) obtained using micro-tensile specimens extracted transversely across the FSP region. In the FSP region, the original sensitized microstructure becomes unsensitized; the unsensitized region is not limited to the friction stir zone but extends outward several mm into the base material. Though the sensitized microstructure is removed, the mechanical testing within the affected area shows the strength and elongation decrease and increase respectively from H116 temper to O temper levels. The previously sensitized microstructure is not observed to have negatively affected the mechanical properties | | | | | |
| 15. SUBJECT TERMS Aluminum Alloys, Friction Stir Processing, Sensitization, Mechanical Testing | | | | | |
| 16. SECURITY CLASSIFICATION OF: | | | 17. LIMITATION OF ABSTRACT SAR | 18. NUMBER OF PAGES 26 | 19a. NAME OF RESPONSIBLE PERSON CAROLINE SCHECK |
| a. REPORT UNCLASSIFIED | b. ABSTRACT UNCLASSIFIED | c. THIS PAGE UNCLASSIFIED | | | 19b. TELEPHONE NUMBER (include area code) 301-227-5144 |

This page intentionally left blank

Contents

| | <i>Page</i> |
|--|-------------|
| Contents | iii |
| Figures..... | iv |
| Tables..... | v |
| Administrative Information | vi |
| Acknowledgements..... | vi |
| Executive Summary | 1 |
| Introduction..... | 1 |
| Experimental Procedure..... | 3 |
| Results and Discussion | 5 |
| Microstructure and Sensitization | 5 |
| Tensile Testing and Fractography..... | 7 |
| Conclusions..... | 11 |
| References..... | 12 |
| Distribution | 1 |

Figures

| | <i>Page</i> |
|--|-------------|
| Figure 1. Micro-tensile and NAMLT specimen locations in relation to the friction stir processed region. The schematic is not to scale..... | 4 |
| Figure 2. Cross-section showing the FSP region microstructure. Close-ups of locations <i>A</i> , <i>B</i> , <i>C</i> , <i>D</i> , <i>E</i> , and <i>F</i> are shown in Figure 3. | 5 |
| Figure 3. Close-ups of locations <i>A</i> , <i>B</i> , <i>C</i> , <i>D</i> , <i>E</i> , and <i>F</i> in Fig 2 are shown clockwise from upper left: a) recrystallized grains within the stir zone, b) interface between the stir zone and TMAZ, c) larger equiaxed grains along the long-transverse direction within the base material, d) the arrows point to intergranular micro-cracking outside the friction stir processed region, e) wormhole defect, and f) small grains in the stir zone above the wormhole defect..... | 6 |
| Figure 4. The results of the NAMLT tests show sensitization levels in the base material and FSP region. Optical microscopy of the etched microstructure shows β phase connectivity varying by distance from the edge of the FSP stir zone. Inset images show microstructure at a) >10mm, b) 10mm, c) 11.5mm, and d) >12mm from the edge of the FSP stir zone. | 7 |
| Figure 5. Tensile properties and fracture modes of the transverse micro-tensile specimens. Five different fracture modes are observed and three of the specimens exhibiting these modes were examined using scanning electron microscopy; the SEM analyzed specimens are identified as <i>A</i> , <i>B</i> , and <i>D</i> . Specimen <i>C</i> was located at the wormhole. Retreating and advancing sides are in relation to the second pass. Referenced H116 and O temper base material values were obtained from bulk (verses micro-tensile) specimens. | 9 |
| Figure 6. The fracture surface and microstructure of specimens <i>A</i> , <i>B</i> , and <i>D</i> are shown from left: a) The failure surface of specimen <i>A</i> exhibits microvoid coalescence. b) Defects are readily observed at the microstructural level in the location of specimen <i>B</i> . c) The V-shaped fracture surface of specimen <i>D</i> at the interface between different microstructures..... | 10 |

Tables

| | <i>Page</i> |
|--|-------------|
| Table 1. Chemical composition of aluminum 5456-H116 (wt. %) | 3 |
| Table 2. Bulk base material properties for H116, O, and sensitized H116 tempered 5456Al | 8 |

Administrative Information

The work described in this report was performed at the Naval Surface Warfare Center, Carderock Division (NSWCCD), West Bethesda, MD in the Survivability, Structures, and Materials Department (Code 60) by the Welding, Processing, and NDE Branch (Code 611). This work was supported by a grant N0001411WX21246 administered by the program manager, Dr. William Mullins, Office of Naval Research Arlington, VA. Dr. Marc Zupan, University of Maryland, Baltimore County (UMBC), Baltimore, MD acknowledges the financial support of the Office of Naval Research (Grant N000141010842 and program manager Dr. William Mullins).

Acknowledgements

The authors would like to thank Stephen Szpara, Rick Stockhausen, and Dr. William Golumbskie for their assistance.

Executive Summary

The microstructures of Al-Mg alloys with greater than 3wt.% Mg can sensitize leaving the material susceptible to intergranular corrosion (IGC); sensitized microstructures are identified by the amassing of β phase precipitates at grain boundaries. Friction stir processing (FSP) has previously been shown to increase the corrosion resistance of sensitized Al-Mg alloys through break-up of the continuous network of β phase particles^[1]. In this study, multi-pass FSP is applied to a sensitized 5456-H116 aluminum plate and the resulting microstructure is linked to local mechanical properties (0.2% yield strength, ultimate tensile strength, and elongation) obtained using micro-tensile specimens extracted transversely across the FSP region. In the FSP region, the original sensitized microstructure becomes unsensitized; the unsensitized region is not limited to the friction stir zone but extends outward several mm into the base material. Though the sensitized microstructure is removed, the mechanical testing within the affected area shows the strength and elongation decrease and increase respectively from H116 temper to O temper levels. The previously sensitized microstructure is not observed to have negatively affected the mechanical properties.

Introduction

Aluminum alloys are used extensively in vehicle applications where designs necessitate high performance without compromising structural component specific strength and stiffness. The direct weight savings obtained by introducing Al, which has a density approximately a third that of steel (2.7g/cm³ compared to 7.8g/cm³ respectively), favorably impacts performance factors including speed, range, payload capacity, and fuel requirements. In 5XXX series Al alloys, Mg and work hardening are used to increase the strength to near low carbon steel levels without significantly decreasing ductility^[1]. Beyond the strength and weight benefits, Al-Mg alloys exhibit excellent general corrosion resistance, weldability, and machinability; these properties have led to Al-Mg alloy usage (particularly 5083Al and 5456Al) in marine environments for Naval applications.

While high levels of Mg contribute to greater strength, the microstructure of alloys with greater than 3wt% Mg are susceptible to sensitization^[2-3]. Sensitization occurs when prolonged exposure to temperatures greater than 50°C causes the precipitation and diffusion of a secondary β phase, (Al₃Mg₂) to the grain boundaries^[2-4]. Over time, the precipitates form a continuous network around the grain boundaries. As the β phase is highly anodic to the Al matrix, in a corrosive environment, intergranular corrosion (IGC) will occur^[4]; the degree to which the microstructure has sensitized is characterized by the resulting mass loss in the material after nitric acid testing.

To treat sensitized microstructures, Al-Mg alloys have been subjected to stabilizing heat treatments that promote the formation of widely spaced globular β phase particles at distance from the grain boundaries. This is achieved by bringing the material above 250°C, the $\beta + \alpha \rightarrow \alpha$

phase transformation temperature for Al-Mg alloys with 4.5wt% Mg, which causes the break-up of the continuous network of β phase particles^[1]. Time and temperature studies using salt baths have shown that exposing highly sensitized microstructures (NAMLT > 100 mg/cm²) to peak temperatures of 266°C or greater leads to an unsensitized microstructure (NAMLT ~2 mg/cm²)^[1]. However, the effectiveness of these treatments over long-term in-service usage and their portability remain problematic^[1,3].

While a sensitized microstructure alone is not problematic, sensitization combined with IGC creates a susceptibility to stress corrosion cracking (SCC) that initiates from tensile stresses in the material in the presence of a corrosive environment. As excessive heating exacerbates the sensitized microstructure while simultaneously introducing tensile stresses into the material, conventional welding procedures have not proven to be effective methods of repairing the cracks in highly sensitized material. To prevent SCC, one or more of the contributing factors (i.e. the susceptible microstructure, corrosive environment, or tensile stresses) must be removed. A potential method for repairing the sensitized microstructure, and thereby increasing the corrosion resistance and removing the ideal crack paths for SCC, is through friction stir processing (FSP).

Friction stir processing is performed on a solid plate with the purpose of modifying the microstructure. Friction stir processing locally modifies the microstructure similar to friction stir welding (FSW) but it does not create a joint. Friction stir welding is a solid state joining process where the material is softened such that the material shear stresses can be overcome by a rotating tool^[5,6]. Because the temperature at which processing occurs is above 250°C, the result is an unsensitized microstructure without geometric change^[1].

The friction stir processed region for Al alloys is generally characterized by a region of refined dynamically recrystallized grains in the stir zone, a thermo-mechanically affected zone (TMAZ), and the heat affected zone (HAZ) which surrounds the TMAZ^[5,7]. Each of these zones displays a unique microstructure resulting in distinct mechanical properties. While previous work has examined the mechanical behavior of FSP Al-Mg alloys^[8,9] and sensitized Al-Mg alloys^[2], and the corrosion behavior of FSP sensitized Al-Mg alloys^[1], no found studies to date have examined the resulting localized mechanical properties of sensitized Al-Mg plate which has been friction stir processed. This study examines the local effects of friction stir processing on sensitized 5456-H116 Aluminum microstructure and the resulting micro-mechanical properties. The material is evaluated through optical metallography (OM), mass loss corrosion testing, micro-tensile specimen testing, and scanning electron microscopy (SEM).

Experimental Procedure

A piece of 5456-H116 Al in-service plate of 6.35mm thickness was used in this study. The material composition was confirmed through direct current plasma emission spectroscopy analysis. The results are shown in Table 1 and were obtained from specimens with dimensions of 12.5mm x 12.5mm x 6.35mm.

Table 1. Chemical composition of aluminum 5456-H116 (wt. %)

| | |
|-------|--------|
| Si | 0.066 |
| Fe | 0.18 |
| Cu | 0.014 |
| Mn | 0.67 |
| Mg | 4.7 |
| Cr | 0.09 |
| Zn | 0.008 |
| Ti | 0.013 |
| Zr | <0.002 |
| Other | <0.015 |

As depicted in Figure 1, a multi-pass friction stir processing with a step-over of a $\frac{1}{2}$ pin length was performed on the Al plate. The locations of the advancing and retreating sides on both the first and second passes are shown in Figure 1. A simple threaded pin of MP-159 tool steel with a 0.205mm length was used. The pin was revolved at 800RPM with a travel speed of 4mm/s and a downward force of 15.57kN. The offset from the center of the first pass to the center of the second pass is 6.45mm.

The sensitization level of the plate was determined through mass loss testing per ASTM G67 *Determining the Susceptibility to Intergranular Corrosion of 5XXX Series Aluminum Alloys by Mass Loss After Exposure to Nitric Acid* (NAMLT Test) in two locations^[10]: in the base metal (85.7mm from the friction stir processing) and at the center of the multi-pass stir zone. Six NAMLT specimens, two in the processed region and four in the base material (the relative locations of which are shown in Figure 1) with dimensions 50mm x 6.35mm x thickness were used.

The friction stir processed material was sectioned using a wire electric discharge machine (EDM) into four 1mm slices at depths of 0.5mm, 1.0mm, 2.5mm, and 3.5mm on the longitudinal plane. Thirty-six micro-tensile specimens (with 1.5mm gage lengths and approximate $250\text{ }\mu\text{m}^2$ cross-sections) were extracted from the layers using a sinker EDM. A Micro Finish Controller was used to minimize the recast layer and the uppermost layers of the specimens were later removed through polishing. Tensile testing was performed at room temperature at a quasi-static strain rate using a mechanical testing system designed for micro-tensile testing. Strain was measured using a non-contact interferometer displacement gage. Readers are directed to Sharpe et. al^[11] and Zupan^[12] for detailed information on interferometer displacement gages and the mechanical testing set-up.

Microstructure etching for both grain boundaries and sensitization was performed using Barker's reagent and a 40% phosphoric etch respectively. Post-fracture fractography was performed using SEM and microstructure analysis was performed using OM.

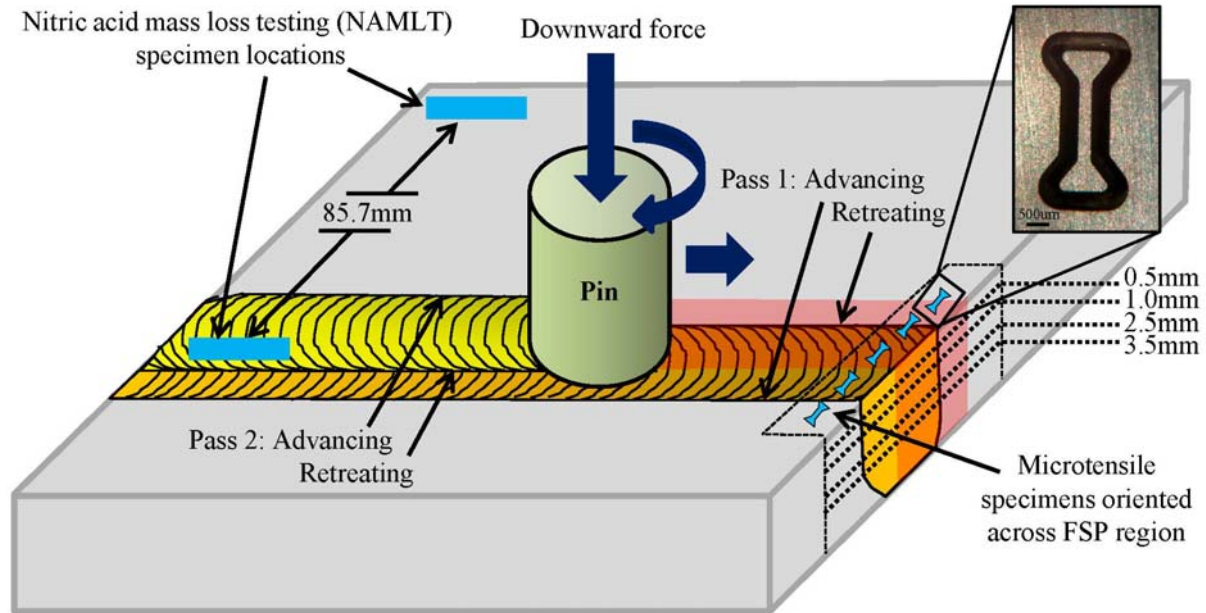


Figure 1. Micro-tensile and NAML specimen locations in relation to the friction stir processed region. The schematic is not to scale.

Results and Discussion

Microstructure and Sensitization

The microstructure of the multi-pass friction stir processed area is shown in Figure 2. The alphabetic labels placed upon the cross-section in Figure 2 present locations where polarized light OM was used to aid in identifying microstructural features as individually presented in Figure 3. The microstructure, on the advancing side of the first pass, clearly defines the location of the rotating pin and the resulting stir zone.

It is noted that the exhibited cross-sectional cut in Figure 2 was photographed several centimeters down the longitudinal length of the processed region from where the microtensile specimen layers were cut. Only the lowest layer of the microtensile specimens (at a depth of 3.5mm) impinged upon the wormhole. Besides the wormhole, volumetric defects are observed on the advancing side of the second pass as well as discontinuities throughout the base material such as small randomly distributed porosity. The volumetric defects are representative of those seen in friction stir processing and friction stir welding.

As shown in Figure 3(a), grains within the friction stir processed area are generally small and round with diameters of 10-20 μm while grains outside the stir zone, shown in Figure 3(c), reach up to 100 μm and are slightly equiaxed in the long-transverse direction. A close-up of the interface at *B* is seen in Figure 3(b) where the smaller recrystallized grains within the stir zone contrast the larger grains within the TMAZ. The microstructure shows the material being swirled upward and pulled into the rotating tool resulting in refined grains. Due to the multi-pass nature of the region, there are no areas showing obvious retreating microstructure. Micro-length intergranular cracking is observed at the extremities of the stir zone as noted by *D* in Figure 2 and in Figure 3(d). Some intergranular cracking outside the stir zone is expected due to the original sensitized microstructure.

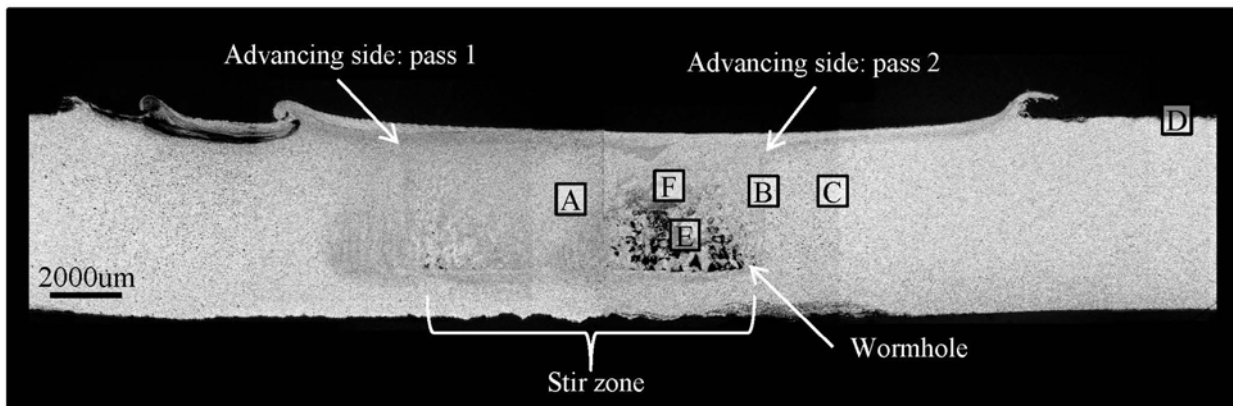


Figure 2. Cross-section showing the FSP region microstructure. Close-ups of locations A, B, C, D, E, and F are shown in Figure 3.

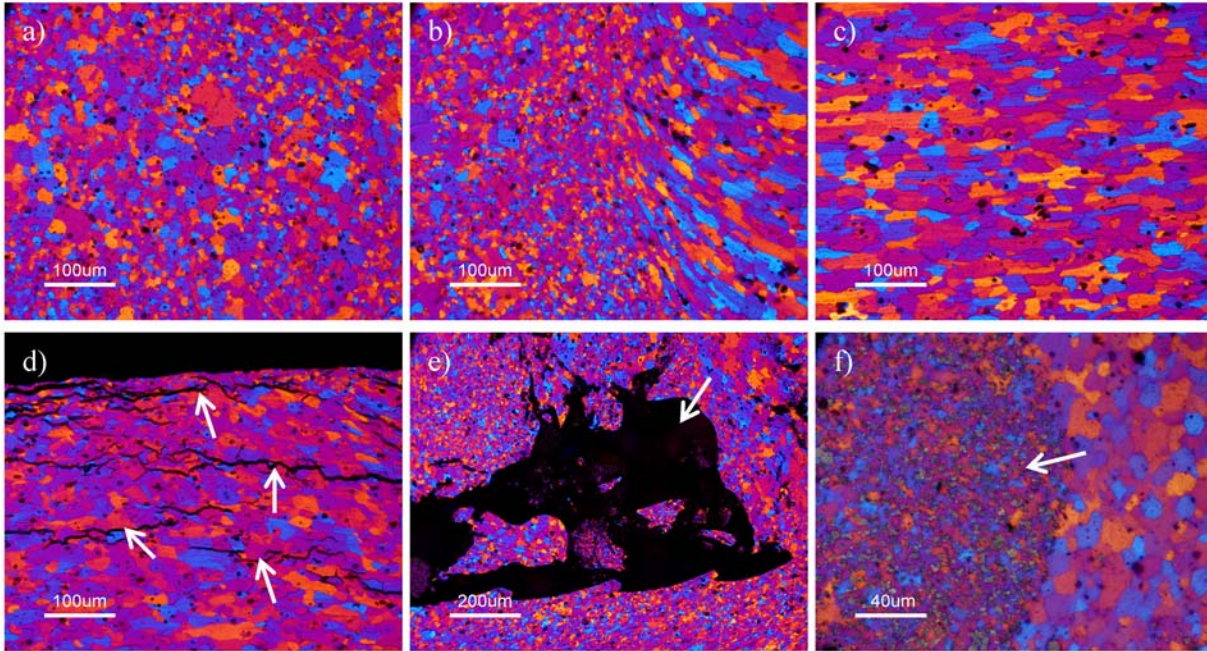


Figure 3. Close-ups of locations A, B, C, D, E, and F in Fig 2 are shown clockwise from upper left: a) recrystallized grains within the stir zone, b) interface between the stir zone and TMAZ, c) larger equiaxed grains along the long-transverse direction within the base material, d) the arrows point to intergranular micro-cracking outside the friction stir processed region, e) wormhole defect, and f) small grains in the stir zone above the wormhole defect.

While the mass loss testing shows an unsensitized microstructure within the FSP region, optical microscopy of etched samples shows repair is not limited to the FSP area, but extends approximately 10mm from the edge of the stir zone into the base material. Etched microstructures showing varying levels of intergranular corrosion are shown in Figure 4(a)-(d). Significant levels of sensitization are seen greater than 12mm from the edge of the stir zone, as shown in Figure 4(d), with a transition to sensitized microstructure occurring from 10mm to 12mm from the edge of the stir zone (Figure 4 (b) and (c) respectively). In this region, the sensitized microstructure is most pronounced along the rolled plane. While β phase connectivity at the grain boundaries is initially observed approximately 11.5mm from the stir zone edge, significant β phase connectivity occurs greater than 12mm from the edge of the stir zone. The size of this repaired microstructural region, being that it is not limited to the immediate FSP zone, is attributed to conductive heat transfer.

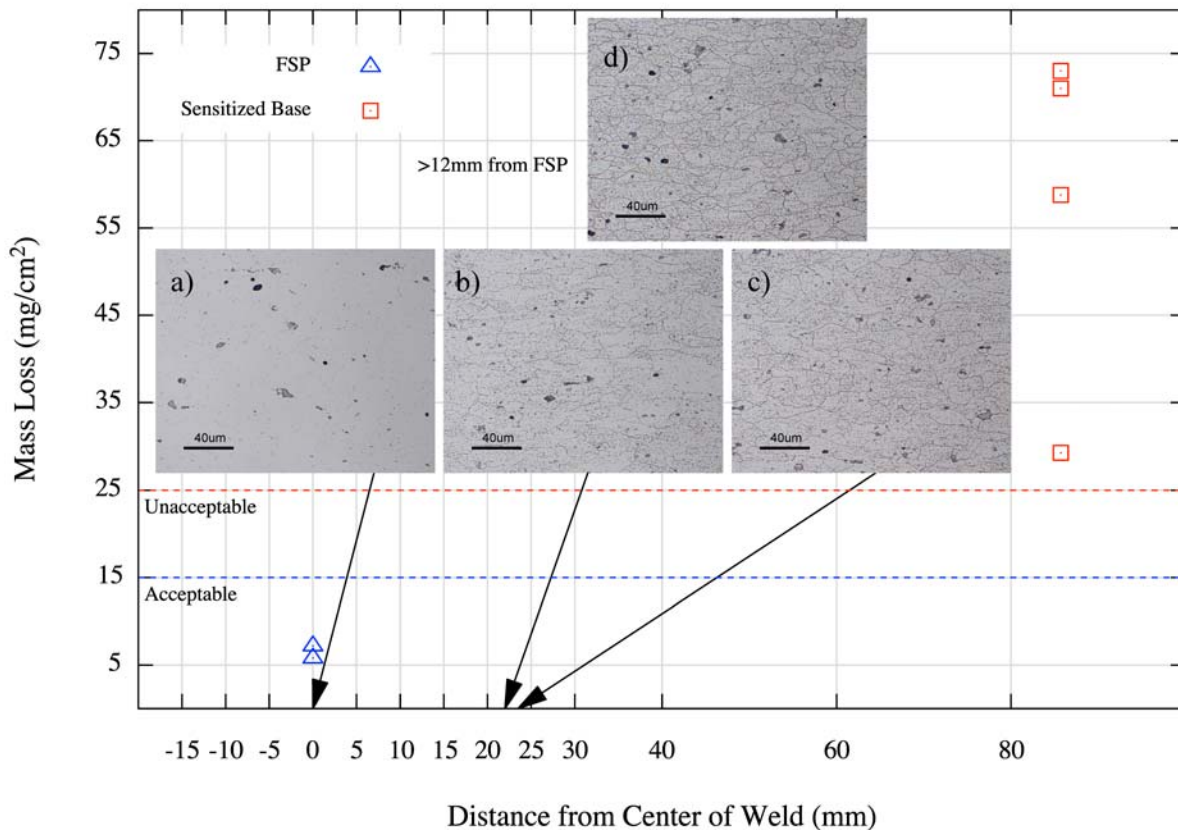


Figure 4. The results of the NAMLT tests show sensitization levels in the base material and FSP region. Optical microscopy of the etched microstructure shows β phase connectivity varying by distance from the edge of the FSP stir zone. Inset images show microstructure at a) >10mm, b) 10mm, c) 11.5mm, and d) >12mm from the edge of the FSP stir zone.

Tensile Testing and Fractography

As the level of sensitization is reduced or unobserved within the stir zone and up to 12mm from the edges, micro-tensile specimens were extracted from this area to evaluate variations in tensile properties across the processed region. The micro-tensile specimens were oriented transversely across the stir zone and extracted at four different depths (0.5mm, 1mm, 2.5mm, and 3.5mm). Specimens were not extracted from the bottommost layer due to the wormhole defect. Referenced H116, O, and sensitized H116 temper base material values were obtained from bulk specimens and are shown in Table 2^[14]; unpublished data provides the mechanical properties for the highly sensitized H116 bulk specimens (NAMLT ~ 57 mg/cm²).

Table 2. Bulk base material properties for H116, O, and sensitized H116 tempered 5456Al

| | UTS (MPa) | YS (MPa) | Elongation % |
|-----------------------------|-----------|----------|--------------|
| H116 temper ^[14] | 352 | 255 | 16 |
| Sensitized H116 temper | 348 | 190 | 23 |
| O temper ^[14] | 310 | 165 | 22 |

The H116 temper is applied to 5XXX Al alloys to increase the strength to levels approaching low carbon steel while maintaining elongations over 10%. While the original base material in this study is 5456-H116 Al, within the region affected by the FSP, the achieved yield and ultimate tensile strengths are reduced to O temper values as shown in Figure 5. The yield strength is reduced an average of 42% and up to 65% over all examined locations from the expected H116 temper value.

Notably, the micro-tensile specimens extracted at different depths (0.5mm and 1.0mm verses 2.5mm and 3.5mm) follow different trends. The average yield strength of the upper two layers of the processed region is 180MPa; this is similar to previously reported transverse properties of macro-scale FSW unsensitized specimens (average yield strength of 175MPa)^[8]. However, the yield strength decreases with increasing depth into the material; a 27% reduction in yield strength occurs over the lower two layers. In the same region, a decrease in the ultimate tensile strength is seen at the advancing edge as well as relative reductions in the center of the stir zone. The advancing edge reductions in strength correlate with the larger grain sizes displayed in the microstructure as seen in Figure 3(b). Particularly noticeable in the lower two layers, the strengths are similar at opposite ends of the processed region; this is expected considering the mirrored microstructure achieved by the multi-pass friction stir processing.

In each layer, the average strain to failure measured post mortem is 23%; this value remains constant regardless of depth or lateral distance from the center of the stir zone and is an increase from the 16% that is expected from H116 base material^[14]. Low elongation values (<10%) are not seen except where specimens were extracted near defects, which would control the failure strain, at the retreating interface, where volumetric defects were identified, and at the wormhole.

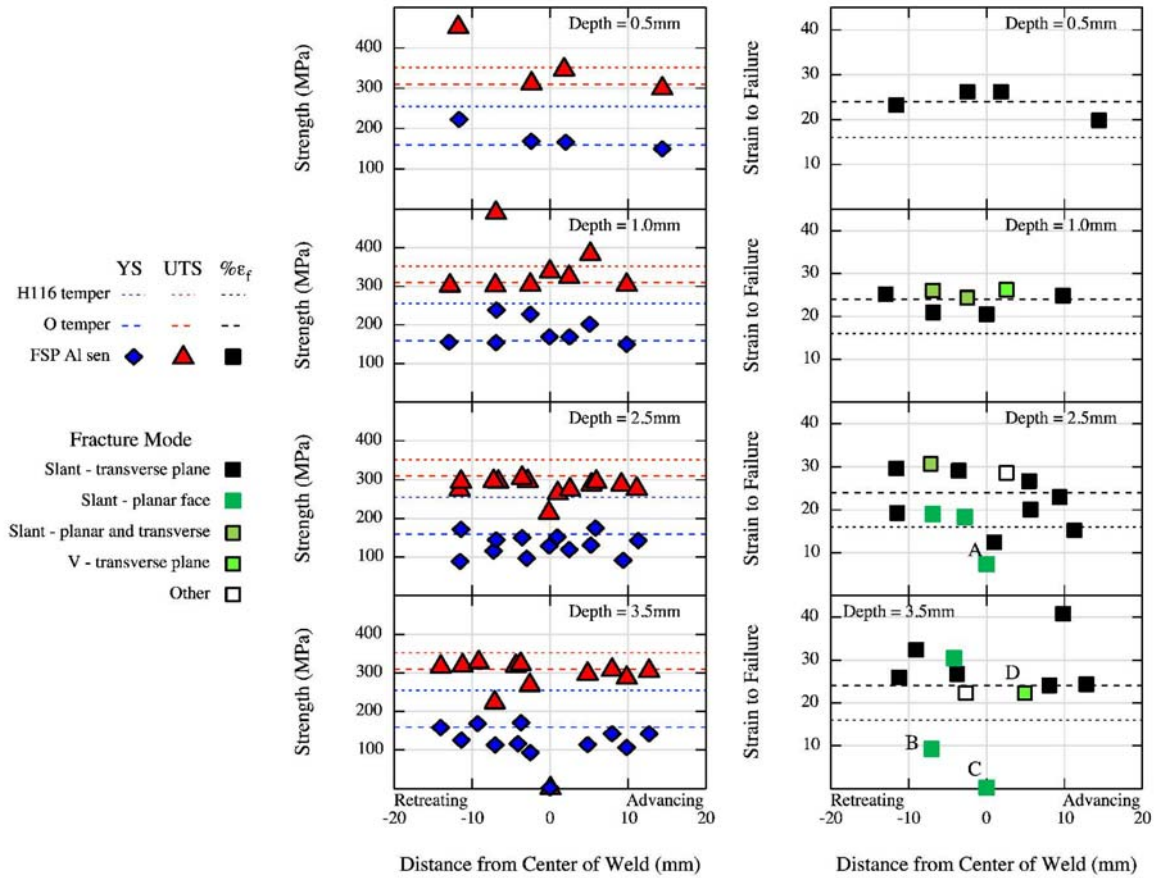


Figure 5. Tensile properties and fracture modes of the transverse micro-tensile specimens. Five different fracture modes are observed and three of the specimens exhibiting these modes were examined using scanning electron microscopy; the SEM analyzed specimens are identified as A, B, and D. Specimen C was located at the wormhole. Retreating and advancing sides are in relation to the second pass. Referenced H116 and O temper base material values were obtained from bulk (verses micro-tensile) specimens.

The fracture modes of the specimens vary by location as shown in Figure 5. The most common fracture mode, exhibited by specimens in all layers, is slanted fracture with microvoid coalescence, such as seen with specimen A in Figure 6(a). Slanted fracture in the specimens occurs due to microstructural asymmetry developed from the processing tool. Due to the similar advancing microstructures at the extremities of the processed area, the same transverse slant fracture characterizes all the specimens at the outer edges of the weld. The slanted failure mode is consistent with work performed by Fonda et. al where macro-scale transversely oriented specimens consistently showed slanted fracture surfaces^[8].

While intergranular cracking within the tested area was not seen, other defects were observed. In Figure 6(b), electron microscopy shows the volumetric defects and foreign particles responsible for initiating the premature failure in specimen *B*. The lowest elongation value is observed in specimen *C* (location shown in Figure 5); the specimen was extracted at the top of the wormhole and was riddled with porosity and cracks. As a result, the specimen failed almost immediately upon loading. A V-shaped fracture surface on the transverse plane is observed in two specimens on the advancing side of the second pass with the fracture surface of specimen *D*, indicated in Figure 5, shown in Figure 6(c). The fracture surface is consistent with the microstructure at the interface between the stir zone and the TMAZ shown in Figure 3(b).

The variations in the specimen fracture modes are expected due to variations in the microstructure from the friction stir processing. There are no indications that the previously sensitized microstructure of the aluminum adversely affected the tensile results. All specimens exhibited fracture surfaces typical of unsensitized friction stir processed Al-Mg alloys and the decrease in strength can be attributed to the processing temperature^[1]. Furthermore, premature failure in the specimens can be linked to the adverse effects of typical FSP defects and not premature or intergranular cracking from intergranular corrosion.

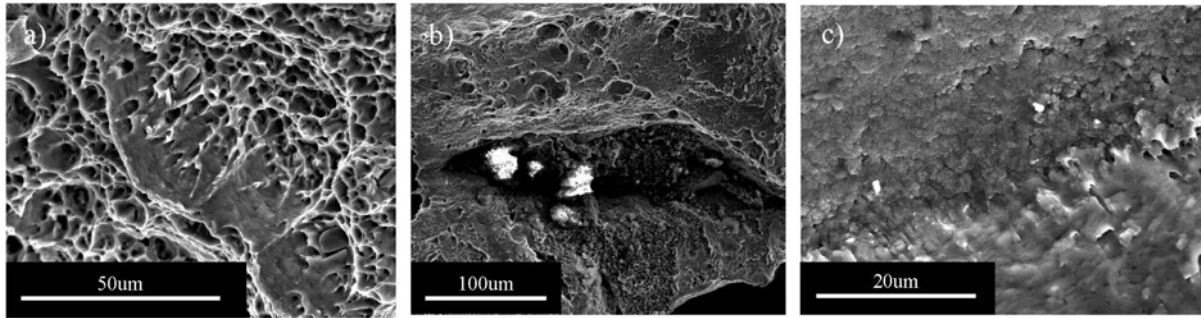


Figure 6. The fracture surface and microstructure of specimens *A*, *B*, and *D* are shown from left: a) The failure surface of specimen *A* exhibits microvoid coalescence. b) Defects are readily observed at the microstructural level in the location of specimen *B*. c) The V-shaped fracture surface of specimen *D* at the interface between different microstructures.

Conclusions

Nitric acid corrosion testing of both base metal and friction stir processed 5456-H116 Al shows friction stir processing effectively repairs the sensitized microstructure. The affected microstructure is not limited to the immediate processing area but extends outward approximately 12mm from the edges of the stir zone. The microstructure defects seen in the stir zone, such as wormholes and volumetric defects near the retreating side on the second pass, are typical defects seen in aluminum friction stir processing and friction stir welding suggesting the previous sensitization does not affect the final microstructure.

There are no indications that the previously sensitized microstructure of the aluminum adversely affected the tensile results.

The tensile testing shows the strength gained from the H116 temper is removed within the heat affected areas. Within the stir zone, the yield strengths are reduced an average of 42% from the expected bulk H116 temper value of 352MPa to the bulk O temper strength. The elongation increases to an average of 23% across the stir zone. The fracture surfaces are typical to aluminum friction stir processing and do not show micro cracking as would be expected in sensitized material.

References

1. A.P. Reynolds and J. Chrisfield: *Corrosion*, 2012, vol. 68, pp. 913-921.
2. I.N.A. Oguocha, O.J. Adigun, and S. Yannacopoulos: *J. Mater. Sci.*, 2008, vol. 43, pp. 4208-4212.
3. L. Kramer, M. Phillippi, W.T. Tack, and C. Wong: *J. Mater. Eng. Perform.*, 2012, vol. 21, pp. 1025-1029.
4. J.L. Searles, P.I. Gouma, and R.G. Buchheit: *Metall. Mater. Trans. A*, 2001, vol. 32, pp. 2859-2867.
5. M.M. Attallah and H.G. Salem: *Mat. Sci. Eng. A-Struct.*, 2005, vol. 391, pp. 51-59.
6. H.B. Chen, K. Yan, T. Lin, S.B. Chen, C.Y. Jiang, and Y. Zhao: *Mat. Sci. Eng. A-Struct.*, 2006, vol. 433, pp. 64-69.
7. R.S. Mishra and M.W. Mahoney: *Friction Stir Welding and Processing*, ASM International, Materials Park, OH, 2007, pp. 71-119.
8. R.W. Fonda, P.S. Pao, H.N. Jones, C.R. Feng, B.J. Connolly, and A.J. Davenport: *Mat. Sci. Eng. A-Struct.*, 2009, vol. 519, pp. 1-8.
9. T. Hirata, T. Oguri, H. Hagino, T. Tanaka, S.W. Chung, Y. Takiawa, and K. Higashi: *Mat. Sci. Eng. A-Struct.*, 2007, vol. 456, pp. 344-349.
10. *ASTM G67 Standard Test Method for Determining the Susceptibility to Intergranular Corrosion of 5XXX Series Aluminum Alloys by Mass Loss After Exposure to Nitric Acid (NAMLT)*, ASM International, West Conshohocken, PA, 2010.
11. D.A. LaVan and W.N. Sharpe: *Exp. Mech.*, 1999, vol. 39, pp. 210-216.
12. M. Zupan and K.J. Hemker: *Exp. Mech.*, 2002, vol. 42, pp. 214-221.
13. A.J. Davenport, M. Jariyaboon, C. Padovani, N. Tareelap, B.J. Connolly, S.W. Williams, and E. Siggs: *Mater. Sci. Forum*, 2006, vol. 519-521, pp. 699-704.
14. *Aluminum and Aluminum Alloys*, ASM International, Materials Park, OH, 1993, pp. 681.

Distribution

DoD CONUS

OFFICE OF NAVAL RESEARCH
ATTN ONR 332 (W MULLINS)
ONE LIBERTY CENTER
875 NORTH RANDOLPH STREET
SUITE 1425
ARLINGTON VA 22203-1995

Copies

1

INTERNAL DISTRIBUTION

Code Name

61

1

611

1

611 (DELOACH)

1

611 (SCHECK)

6

612 (ROE)

1

614 (DUCKWORTH)

1

Copies

This page intentionally left blank

